

## DOMAIN STABILITY IN PZT THIN FILMS

## DOMAIN STABILITY IN PZT THIN FILMS

GRADY S. WHITE, JOHN E. BLENDELL, and EDWIN R.  
FULLER, JR.

National Institute of Standards and Technology  
100 Bureau Drive Stop 8522, Gaithersburg, MD 20899

AFM measurements were made on  $\langle 111 \rangle$  textured lead zirconate titanate thin films excited by a  $1 V_{\text{rms}}$  in the presence of various DC biasing voltages. Domain pinning sites were found in the film. All sites were located at grain boundaries and were coincident with abnormally large piezoelectric displacements in the film. Different sites were associated with domain polarization aligned toward the free surface of the film than with polarization aligned toward the substrate. Finite element calculations used to determine residual stress as a function of grain misorientation showed that large residual stresses and strains normal to the film plane would be generated at grain boundaries for certain grain misorientations. Domain pinning sites in PZT thin films are interpreted in terms of residual stresses at grain boundaries due to grain misorientation.

Keywords AFM; domain; ferroelectric; grain boundary; pinning; PZT

### INTRODUCTION

Domain pinning in ferroelectric films has been attributed to a number of causes, e.g., oxygen vacancies [1-3], point defects [4], and extended defects [5]. In addition, defect locations have been assigned to domain walls [6], grain boundaries [4] and the film-substrate interface [7]. While charged defects will clearly interact with domains, other microstructural aspects of a polycrystalline film might also affect domain motion. In particular, local residual stress formed near grain boundaries as a function of the crystallographic misorientation across

their common grain boundary could affect domain mobility by changing unit cell dimensions and, perhaps, through biasing defect trap depths.

Atomic force microscopy (AFM) is a tool [8,9] that has proven very valuable for monitoring local domain behavior of ferroelectric films in the presence of external fields [10-15]. Using AFM techniques, we present evidence of domain pinning in a ferroelectric film and give results of a finite element (FE) analysis that estimate residual stresses arising from grain-to-grain misorientations.

## PROCEDURE

### Experimental

An unpoled  $\text{Pb}(\text{Zr}_x\text{Ti}_{1-x})\text{O}_3$  (PZT) film, courtesy of Y.E. Lee (Seoul National University) was deposited by rf magnetron sputtering of PZT and Pb targets onto a  $\text{Si}/\text{SiO}_x/\text{Ti}/\text{Pt}/\text{TiO}_x$  substrate. The film was  $\approx 350$  nm thick with a mean grain size of 250 nm, determined by the linear intercept length technique and textured with the  $\langle 111 \rangle$  axis normal to the film plane (x-ray rocking curve FWHM =  $2.4^\circ \pm 0.1^\circ$ ). Cross-section transmission electron microscopy (TEM) of similar films suggested that the film was one grain thick.

A commercial atomic force microscope<sup>#</sup> (AFM) operating in contact mode with a Co-coated Si tip was used to monitor film topography and piezoelectric response. A variable power supply\* provided  $1\text{V}_{\text{rms}}$  excitation at 7 kHz and up to  $\pm 6\text{V}_{\text{dc}}$  bias voltage across the film. The AFM tip and the Pt beneath the PZT film acted as electrodes. The signal from the position sensitive detector in the AFM was analyzed with a digital, vector lock-in amplifier<sup>†</sup>. Both magnitude and phase of the piezoelectric response of the film were measured simultaneously with the film surface topography. Phase measurements provided image contrast between dipoles aligned away from the substrate and those aligned toward the substrate. Magnitude

---

<sup>#</sup> Nanoscope IIIa, Model NS3a & ADCS, Digital Instrument, Veeco Metrology Group, Santa Barbara, CA. Trade names are given to provide complete experimental description and are not intended as an endorsement by the National Institute of Standards and Technology.

\* Wavetek Function Generator, Model 21, Wavetek/datron, San Diego, CA

<sup>†</sup> Stanford Research Systems Model SR850 DSP Lock-In Amplifier, Stanford Research Systems, Sunnyvale, CA

## DOMAIN STABILITY IN PZT THIN FILMS

measurements provided a map of piezoelectric-driven displacement normal to the plane of the film.

### Modeling

A two-dimensional FE code [16] was used to model the stresses associated with grain misorientations in plane strain mode. Only stresses resulting from mechanical constraints were considered; electric field effects were not included in these calculations. Stresses were generated by converting the grains from cubic to tetragonal symmetry; the  $c/a$  ratio in the tetragonal grains was set at 1.02, similar to a bulk hard PZT.

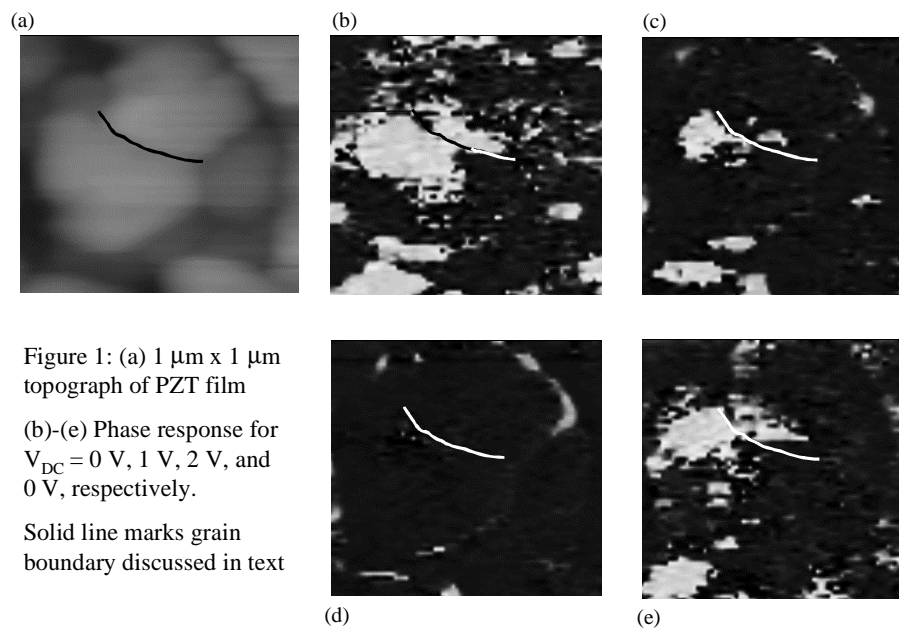
For the first set of calculations, the elastic constants used were:  $c_{11} = 156$  MPa,  $c_{12} = 88.6$  MPa,  $c_{13} = 84.5$  MPa,  $c_{33} = 130$  MPa,  $c_{44} = 25.6$  MPa, and  $c_{66} = 100$  MPa, again, mimicking a hard PZT. The geometry used in the calculations consisted two grains separated by a grain boundary. Grains were defined to be 170 nm thick and 400 nm wide. The bottoms of the grains (i.e., the film/substrate interface) were fixed while sides and top surfaces were free to distort. The grains were wide enough to minimize edge effects on the calculated stress values at the central grain boundary. Only the center 400 nm (200 nm width of the grains on each side of the grain boundary) section is plotted here.

All calculations were made with the [111] crystal axes normal to the film plane (the  $+\hat{y}$  direction in the lab frame). The orientation of the right-hand grain was fixed. The left-hand grain was rotated about the [111] crystallographic axis in approximately  $22^\circ$  increments. Initially, both grains were oriented with the [111] and [001] axes in the plane of the paper, with the [001] axes directed up and to the right. After each rotation, the system was allowed to equilibrate and the stress tensor,  $\sigma$ , was calculated as a function of position within the grains.

For the second set of calculations, a row of six grains, 350 nm wide by 350 nm thick, was used. For these calculations, the projection of the  $c$ -axis in the plane of the film for each grain was aligned (from the left-hand grain to the right-hand grain) in the  $+\hat{z}$ ,  $+\hat{x}$ ,  $-\hat{x}$ ,  $+\hat{x}$ ,  $-\hat{x}$ , and  $+\hat{z}$  directions. The boundary conditions for these calculations were identical to those of the first calculation, but, for simplicity, isotropic elastic constants (100 MPa) were used.

RESULTS AND DISCUSSION

Figure 1a shows a topograph of several grains and grain boundaries. Figures 1b-1e are phase images of the same region, made as a function of bias voltage,  $V_{dc}$ . Overlaid on Figs. 1b-1e is the curved grain boundary outlined in Fig. 1a. For Fig. 1b,  $V_{dc} = 0$ . The fact that the image shows



similar amounts of light and dark areas suggests that, at  $1\ V_{rms}$ , the alternating electric field is not large enough to switch domain orientations. When a one-volt bias voltage is added, Fig. 1c, the relative fraction of the light regions is reduced significantly as domains switch to align with the bias field. Of particular interest in Fig. 1c is the bright region that was at the center of the large bright area in Fig. 1b. This region is a remnant of the earlier, larger domain that was oriented opposite to the applied field; the remaining, unswitched domain area in Fig. 1c has been reduced to a smaller area adjacent to the grain boundary. When  $V_{dc}$  is increased to  $+2\ \text{V}$ , Fig 1d, this entire region switches to align with the bias field. When  $V_{dc}$  is returned to zero, the domains along the highlighted grain boundary switch back to their original alignment. It is interesting that, even at  $V_{dc} = 2\ \text{V}$ , there are still unswitched regions in Fig. 1d. All of the unswitched regions lie along grain boundaries and are subsets of larger unswitched regions

## DOMAIN STABILITY IN PZT THIN FILMS

seen in Fig. 1 c which are themselves subsets of bright regions shown in Fig. 1b. It should be noted that not all of the grain boundaries in Fig. 1 exhibit this strong resistance to switching that we are equating to domain pinning.

Measurements of these and other areas indicate that domain switching is not a random event. Instead, as the bias voltage is increased, the areas containing unswitched domains decrease in size with the last regions to switch being adjacent to certain grain boundaries. As  $V_{dc}$  is reduced, the domains switch back to their original configurations, expanding out from the grain boundaries as a function of the reduced bias voltage. This behavior has been observed with approximately equal frequency for both  $\pm V_{dc}$ . To date, no overlap has been observed in pinning regions for  $+V_{dc}$  and  $-V_{dc}$ .

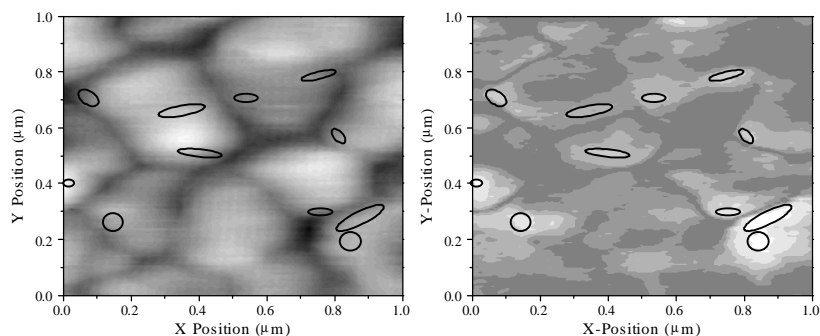
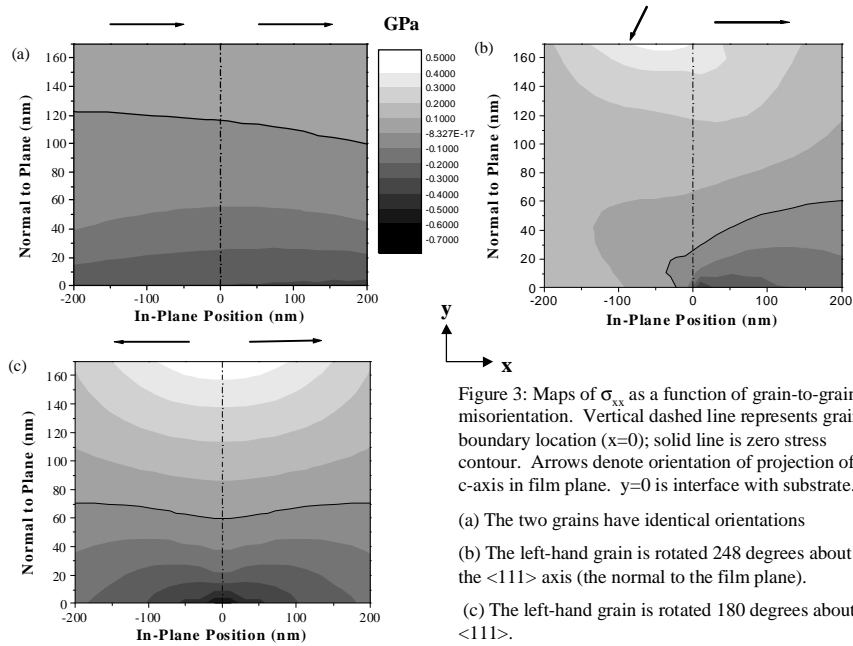


Figure 2: (a) Topographic map of grain structure. (b) Corresponding map of the magnitude of the piezoelectric response normal to the film surface. Light regions in (b) correspond to larger displacements. The large displacements correspond almost exclusively to edge of grain locations (note circled regions).

Fig. 2a shows grain morphology for another region of the film and Fig. 2b maps the magnitude of the piezoelectric response normal to the plane of the film in the presence of  $V_{dc} = -2V$ . The magnitude is essentially uniform except for a number of areas that show unusually large extension. Comparison with Fig. 2a shows that these regions are all adjacent to grain boundaries. Corresponding maps of the piezoelectric displacement show that almost all of the regions of large displacement map onto phase images in which the domains are pinned, either up or down.

While the behavior shown in Fig. 1 shows that grain boundaries can play a major role in pinning in domains in PZT thin films, the

mechanism that pins the domains remains unknown. However, there are several features that suggest that grain misorientation plays a role. First, the observation that not all grain boundaries appear to affect the domains indicates that there are distinct differences in behavior for different grain boundaries or different regions of the same grain boundary. Second, observation shows that some grain boundary locations pin domains with their dipoles oriented away from the substrate while others pin the domains with their dipoles directed toward the substrate. This suggests that charge compensation along grain boundaries for charge injection between the film and substrate is



not an explanation for the observed pinning, since that would be expected to be a unidirectional process. Third, the abnormal displacement seen in Fig. 2 is consistent with lateral mechanical constraints at certain grain boundaries. The coincidence of those locations with domain pinning sites implies that the microstructural features giving rise to the constraints might also play a role in the pinning. An obvious candidate to generate mechanical constraints at various locations in the film is grain misorientation. A random distribution of grain orientations within the plane of the film would be

## DOMAIN STABILITY IN PZT THIN FILMS

consistent with the observation that certain grain boundaries appear to pin domains and others do not.

One result of grain-to-grain misorientation is residual stress generation at the grain boundary. Consequently, we have calculated residual stresses resulting from grain misorientation using the geometries and boundary conditions described previously. If residual stresses resulting from grain misorientation are a partial explanation for domain pinning, based upon the experimental results described above, there must be certain grain-to-grain orientations that generate large stress while, for other orientations, the grain boundary stresses should remain fairly small. In addition, there must be unusually large displacements at high stress grain boundaries.

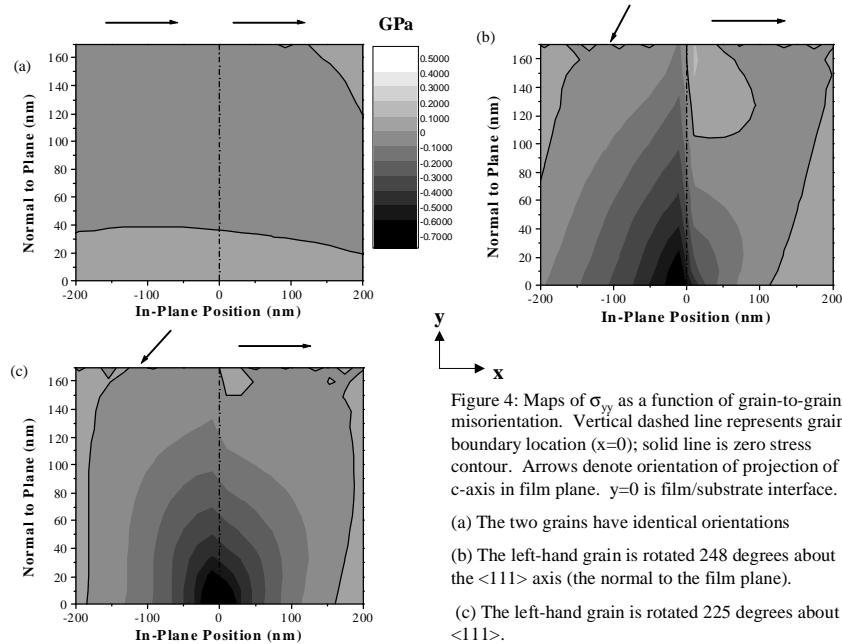


Figure 4: Maps of  $\sigma_{yy}$  as a function of grain-to-grain misorientation. Vertical dashed line represents grain boundary location ( $x=0$ ); solid line is zero stress contour. Arrows denote orientation of projection of c-axis in film plane.  $y=0$  is film/substrate interface.

Figure 3 maps  $\sigma_{xx}$  for three different grain misorientations. The vertical dashed line in the center of each image represents the grain boundary. In all cases,  $\langle 111 \rangle$  is parallel to  $\hat{y}$ . The arrows above the maps are projections of the c-axis in the film plane. Because the calculations include only mechanical stresses, they are identical for  $180^\circ$  dipole switches; the purpose of the calculations is strictly to determine the level and distribution of residual stresses arising elastically from misorientations between two grains. In Fig. 3a, there

is no misalignment. Both c-axes point to the right and upward. Values of  $\sigma_{xx}$  are quite low, being slightly tensile near the top of the grains and becoming compressive as the substrate is approached. Since the orientations of the two grains are identical, the stresses are not affected by the grain boundary. As the left-hand grain rotates relative to the right hand grain,  $\sigma_{xx}$  becomes more complicated and the grain boundary becomes important. For a rotation about  $\langle 111 \rangle$  of  $248^\circ$ , Fig. 3b, the stress becomes predominately tensile in both grains, although the stress distribution is quite nonuniform. Adjacent to the grain boundary at the top of the grains (“film surface”), the left-hand grain experiences a tensile stress  $> 0.4$  GPa. Simultaneously, a compressive stress builds at the interface with the substrate adjacent to the grain boundary in the right-hand grain. Here,  $|\sigma_{xx}| > 0.4$  GPa. The maximum stresses remain about constant as the rotation of the left-hand grain continues, but the stress distribution becomes symmetric about the grain boundary (see Fig. 3c).

Values of  $\sigma_{yy}$  for the same conditions are shown in Figure 4. Again, when the two grains are aligned, the stresses are quite low,  $|\sigma_{yy}| \leq 0.1$  GPa. As the left-hand grain is rotated, stresses build, especially along the grain boundary. These stresses are predominately compressive but around  $248^\circ$  regions of small tensile stress, less than 0.2 GPa, occur near the surface in the right-hand grain (Fig. 4b). At the same time, compressive stresses  $> 0.8$  GPa are generated at the left-hand side of the grain boundary at the film/substrate interface. As the left-hand grain is rotated further, the tensile region disappears almost completely and the compressive region becomes centered on the grain boundary (Fig. 4c). The lack of a significant tensile stress region in  $\sigma_{yy}$  results from the fact that the film surface is free to distort although the film/substrate interface is clamped.

Figure 5 plots the distortion ( $\times 20$ ) of the row of grains described in the modeling section in which the c-axis orientations are chosen to generate maximum  $\sigma_{xx}$  tensile (c-axes away from each other) and compressive (c-axes toward each other) stress. Surface displacement in these two orientations is minimum or maximum, respectively, at the grain boundaries. The presence of a driving voltage,  $V_{ac}$ , would cause an enhanced displacement at these grain boundaries.

## DOMAIN STABILITY IN PZT THIN FILMS

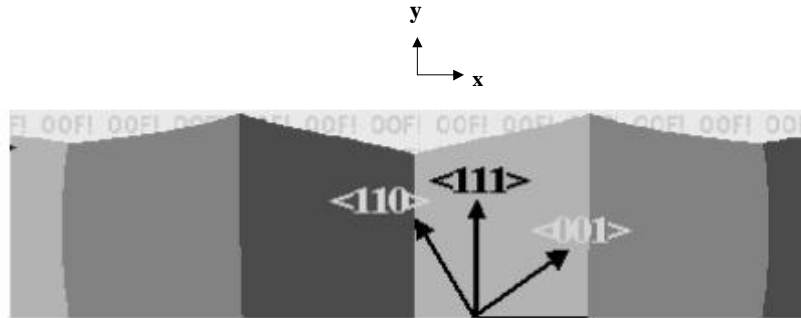


Figure 5: Two dimensional finite element calculation of distortion (expanded by x20) resulting from cubic to tetragonal transformation. Peaks correspond to adjacent grain c-axes pointed towards each other.

In synopsis, the FE calculations show, for grain misorientations less than about  $90^\circ$ , mechanically induced residual stresses are fairly small, i.e. on the order of a hundred MPa. For larger misorientations, stresses exceed 0.5 GPa in both compression and tension for  $\sigma_{xx}$  and surpass 0.7 GPa in compression for  $\sigma_{yy}$ . These calculations show that certain misorientations result in larger piezoelectric extension at the grain boundaries than in the center of the grains. The FE calculations are consistent with all of the features observed experimentally.

### SUMMARY AND CONCLUSIONS

AFM measurements of a PZT thin film excited at  $1 V_{\text{rms}}$  in the presence of various DC biasing voltages detected apparent domain pinning sites in the film. The sites were located at grain boundaries and were coincident with abnormally large piezoelectric displacements. Experimental observations were correlated with FE calculations that showed large residual stresses and normal strains would be generated at grain boundaries for specific grain misorientations. These results suggest that residual stresses generated at grain boundaries by grain-to-grain misorientation in PZT thin films play an important role in domain pinning.

REFERENCES

1. I.K. You, S.B. Desu, and J.Xing, MRS Symp. Proc. **310** 165 (1993).
2. M. Dawber and J.F. Scott, Appl. Phys. Lett. **76** (8) 1060 (2000).
3. K. Niwa, Y. Katoka, M. Tomotani, H. Ashida, Y. Goto, and S. Otani, Acta mater. **48** 4755 (2000).
4. W.L. Warren, D. Dimos, B.A. Tuttle, R.D. Nasby, and G.E. Pike, Appl. Phys. Lett. **65** (8) 1018 (1994).
5. J.F. Scott and C.A. Paz de Araujo, Science **246** 1400 (1989).
6. W.L. Warren, D. Dimos, B.A. Tuttle, R.D. Nasby, and G.E. Pike, Appl. Phys. Lett. **65**, 1018 (1994).
7. E.L. Colla, D.V. Taylor, A.K. Tagantsev, and N. Setter, Appl. Phys. Lett. **72** (19) 2478 (1998).
8. A. Gruverman, O. Auciello, and H. Tokumoto, J. Vac. Sci. and Tech. B, **14** (2) 602 (1996).
9. G. Zaval, J.H. Fendler, and S. Trolier-McKinstry, J. Appl. Phys. **81** (11) 7480 (1997).
10. P. Güthner and K. Dransfeld, Appl. Phys. Lett. **61** (9) 1137 (1992).
11. T. Hidaka, T. Maruyama, M. Saitoh, N. Mikoshiba, M. Shimizu, T. Shiosaki, L.A. Wills, R. Hiskes, S.A. Dicardis, and J. Amano, Appl. Phys. Lett. **68** (17) 2358 (1996).
12. A. Gruverman, O. Auciello, R. Ramesh, and H. Tokumoto, Nanotechnology **8** A38 (1997).
13. C.S. Ganpule, V. Nagarajan, S.B. Ogale, A.L. Roytburd, E.D. Williams, and R. Ramesh, Appl. Phys. Lett. **77** (20) 3275 (2000).
14. A. Roelofs, U. Böttger, R. Waser, F. Schlaphof, S. Trogisch, and L.M. Eng, Appl. Phys. Lett. **77** (21) 3444 (2000).
15. D. Bolten, U. Böttger, T. Schneller, M. Grossmann, O. Lohse, and R. Waser, Appl. Phys. Lett. **77** (23) 3830 (2000).
16. S.A. Langer, E.R. Fuller, Jr., and W.C. Carter, accepted for publication Computing in Sci. and Eng. (May/June2001).